Journal of Chromatography A, 1217 (2010) 1934–1941

Contents lists available at ScienceDirect

Journal of Chromatography A

journal homepage: www.elsevier.com/locate/chroma

The direct inverse method: A novel approach to estimate adsorption isotherm parameters

Jeroen Cornel[a], Abhijit Tarafder[b], Shigeharu Katsuo[a], Marco Mazzotti[a,*]

[a] Institute of Process Engineering, ETH Zurich, Sonneggstrasse 3, 8092 Zurich, Switzerland
[b] Institute of Chemical and Bioengineering, ETH Zurich, Wolfgang-Pauli-strasse 10, 8093 Zurich, Switzerland

ARTICLE INFO

Article history:
Received 3 November 2009
Received in revised form 17 January 2010
Accepted 19 January 2010
Available online 25 January 2010

Keywords:
Adsorption isotherms
Liquid chromatography
Inverse method
Optimization
Calibration-free

ABSTRACT

A novel method to estimate adsorption isotherm parameters is presented and its applicability is studied through synthetic as well as experimental data. This approach assumes a linear dependency of the UV absorption intensity on the solute concentration in the fluid phase, at least in certain ranges of the UV spectra. It was demonstrated that by fitting the absorption profiles, i.e. the new direct inverse method, and by fitting the concentration profiles, i.e. the classical inverse method, very similar adsorption isotherm parameters can be obtained. The findings presented in this work have as important implication the elimination of the requirement of converting a measured absorption intensity into a concentration value, i.e. the elimination of the calibration of the UV signal.

1. Introduction

Liquid chromatography is frequently applied as a chemical separation process to isolate one or more components from a mixture. Its separation mechanism is a consequence of the difference between the retention characteristics of the individual components in the mixture. Elucidation of the adsorption isotherms and estimation of their parameters is a crucial step towards designing an optimal preparative chromatographic process.

Several methods exist to characterize adsorption isotherms through chromatography, among them frontal analysis and the perturbation method [1]. These methods can be used to estimate single as well as multi component isotherms and require a significant amount of experimental effort and material.

One method that allows estimation of single and multi component competitive isotherm parameters with little experimental effort, is the inverse method or classical inverse method (CIM) as it is referred to throughout this work. In this method, the adsorption isotherm parameters are obtained by fitting simulated chromatograms to experimental ones. This method has successfully been applied to determine adsorption isotherm parameters for many species using various adsorption isotherms [1–7]. However, there are several drawbacks of this classical inverse method. In all cases, the signal of the detector, e.g. an ultraviolet (UV) spectrometer, requires calibration, which is a time-consuming and costly exercise. In the case where components are overlapping, two options to apply the classical inverse method exist. The first is a fraction collection and subsequent analysis of these fractions, which by itself also requires calibration of the UV signal. This allows obtaining the elution profiles of the individual components and facilitating the application of the classical inverse method. The second option is to use the calibration and the simulated concentration profiles to calculate the response of the detector, which is typically related to the sum of the concentrations of all the species present, and to fit this to the measured response [5,6]. Both options require a calibration for each component at one or at multiple wavelengths, hence they require either significant quantities of pure components, i.e. a critical requirement in an industrial environment, or additional calculations to estimate the calibration factors from a series of measurements using mixtures of known concentrations at different dilutions.

In this work, a novel method to estimate adsorption isotherm parameters, the direct inverse method (DIM), is presented. The proposed approach is a modification of the classical inverse method and uses directly the elution profiles at multiple wavelengths provided by the UV spectrometer or detector without any calibration efforts. Moreover, the operating principles of the DIM are equally applicable in the case of strongly overlapping components and therefore they eliminate the necessity of fraction analysis, which is also very time-consuming. It is worth noting that both the classical and the direct inverse method require the selection of a specific isotherm, i.e. a specific functional form to describe adsorption.

* Corresponding author. Tel.: +41 44 6322456; fax: +41 44 6321141.
E-mail address: marco.mazzotti@ipe.mavt.ethz.ch (M. Mazzotti).

0021-9673/$ – see front matter © 2010 Elsevier B.V. All rights reserved.
doi:10.1016/j.chroma.2010.01.063

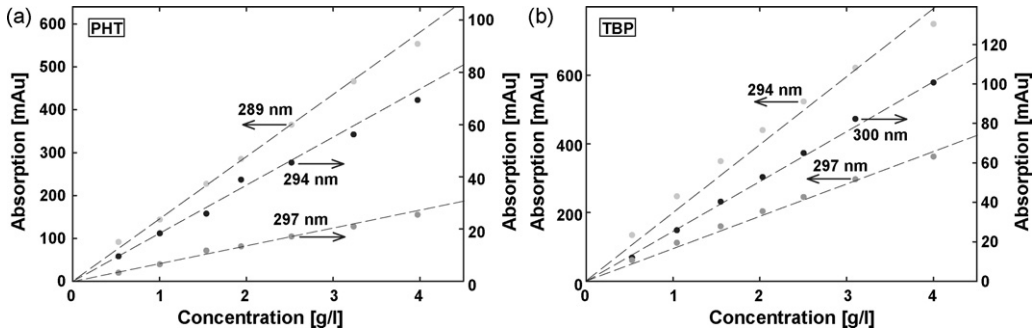

Fig. 1. UV intensity as a function of the solute concentration in the fluid phase in the case of phenetole (component 1) in part a and of 4-*tert*-butylphenol (component 2) in part b, respectively. All measurements were performed at 22 °C by injecting 5 mL of the solution without the installation of a column and the values shown are the values of the resulting plateaus. Please note that the arrows indicate the different scales for the *y*-axis.

Such a choice can be made based on a series of overloaded pulse injections starting with the simplest isotherms and using more complicated ones when necessary [1].

It is known that the adsorption isotherm parameters estimated through the inverse method are accurate only up to the concentration levels reached at the column outlet in the experiments considered for the parameter estimation [1]. This is true also for the proposed direct inverse method. Alternative approaches to overcome this limitation are of course possible, which are based on frontal analysis or variations thereof [1,8].

The direct inverse method has similarities with a recent study that estimates the adsorption isotherm parameters using the sum of the concentrations of two enantiomers [3]. The method proposed in that work however, works only in the case of enantiomers, which have of course identical UV spectra, and still requires calibration. In two other publications, the sum of the absorptions is used to estimate the concentrations of two components having different UV spectra through the solution of an optimization problem [5,6]. Also in those studies, a calibration for each component was required. The novel direct inverse method works in both cases, i.e. for enantiomers and for components that have different UV spectra, does not require calibration, and therefore does not require any quantities of pure components for its application.

The main assumption of the proposed direct inverse method is that for all the involved components, the measured UV absorption scales linearly with the solute concentration in the fluid phase. It is known that this is certainly not the case for all the wavelengths, however over small ranges the absorption increases linearly with the solute concentration in the fluid phase as it is shown in Fig. 1(a) and (b) for the two components used in this work, i.e. phenetole (PHT) and 4-*tert*-butylphenol (TBP), respectively.

In this paper, first synthetic data is used to demonstrate the effectiveness of this novel method. Subsequently, experimental data are used to show that very similar adsorption isotherm parameters can be obtained when fitting directly the time-resolved UV spectra and when fitting the time-resolved concentrations of the individual components. These elution profiles are obtained either through calibration of the UV signal or through fraction analysis in the case of overlapping components.

As any other method to estimate adsorption isotherm parameters, the proposed direct inverse method has advantages and disadvantages. On the one hand, it is clear that the assumption of linearity between concentration and UV absorbance limits the applicability of the proposed method to a certain range of wavelengths. On the other hand, the method is calibration-free and does not require the pure components to be available. This method can be seen as an additional method to estimate adsorption isotherm parameters, which has obvious advantages and can be applied when the relationship between concentration and detector response is linear. To the best of the authors' knowledge, a calibration-free modification of the classical inverse method that can be applied also to multi component mixtures has never been reported.

2. Experimental

2.1. System

All data was acquired using an Agilent (Palo Alto, CA, USA) LC System 1100 Series equipped with a multisolvent delivery system, an auto-sampler, a column thermostat, a diode array UV detector and an automated data acquisition system. The extra-column volume was 0.078 mL and has been accounted for in all data reported. In all the experiments, the temperature in the column thermostat was kept constant at a value of 22 °C. The flow rate in all the experiments was 1 mL/min.

2.2. Chemicals

Phenetole or ethoxybenzene and 4-*tert*-butylphenol were purchased from Sigma–Aldrich (Buchs, Switzerland) and used without further purification. Uracil or 2,4-dihydroxypyrimidine, also purchased from Sigma–Aldrich, was used as a tracer to determine the extra-column volume of the system and the overall bed void fraction of the column. A methanol–water mixture (65:35, v/v) was used as the mobile phase in all the experiments. Deionized water was obtained from a Milli-Q Advantage A10 water purification system from Millipore (Zug, Switzerland) and HPLC grade methanol was purchased from Sigma–Aldrich.

2.3. Column

The chromatographic column used was a C18 Zorbax-StableBond300 from Agilent (150 × 4.6 mm). The column overall bed void fraction was estimated to be 0.62 using uracil as a tracer compound. During the experiments, fractions were collected using a FC203B fraction collector from Gilson (Mettmenstetten, Switzerland).

3. Modeling the spectroscopic data

3.1. Notation

In this section, the proposed method to estimate adsorption isotherm parameters, i.e. the direct inverse method, will be discussed in detail. The proposed method is similar to a novel approach to estimate kinetic parameters from Raman or infrared spectra

applied to a crystallization process [9,10], and hence a very similar notation will be used.

We assume that the measured UV spectra, which were used without any preprocessing, scale linearly with the concentration of all d components. The measured signal intensity at a certain wavelength λ and at a given time t, $x(t, \lambda)$, can then be expressed as a linear combination of the signals corresponding to each component, i.e.:

$$x(t, \lambda) = \sum_{l=1}^{d} c_l(t) a_l(\lambda) + e(t, \lambda) = \hat{x}(t, \lambda) + e(t, \lambda) \quad (1)$$

where $a_l(\lambda)$ represents the intensity at wavelength, λ, of the pure-component spectrum corresponding to the lth component, $c_l(t)$ denotes the concentration of the lth component at time t, and $e(t, \lambda)$ represents the experimental error, i.e. due to the noise and the non-idealities of the measurement. By discretizing the spectral and the time coordinates, the spectral matrix $\mathbf{X}$ $(n \times m)$ can then be written as:

$$\mathbf{X} = \mathbf{CA} + \mathbf{E} = \hat{\mathbf{X}} + \mathbf{E}. \quad (2)$$

The element x_{ij} of the matrix $\mathbf{X}$ represents the jth measured intensity for the ith sample and $\mathbf{C}$ $(n \times d)$ represents the state matrix, i.e. the concentrations of the d components involved, where the lth column of $\mathbf{C}$ is the discretized concentration profile in time of the lth component. The lth row in the matrix $\mathbf{A}$ $(d \times m)$ denotes the discretized pure-component spectrum for component l; the matrix $\mathbf{E}$ $(n \times m)$ is the matrix of experimental errors. It is worth noting that the discretization of the wavelength coordinate as well as the sampling in time are determined by the settings of the instrument, i.e. the spectrometer.

3.2. Classical inverse method

In the classical inverse method, the adsorption isotherm parameters are obtained by fitting simulated chromatograms, i.e. the time-evolution of the concentrations of the individual components, to the experimental ones. Therefore, the CIM requires a calibration of the UV signal that converts the time-evolution of the intensity at one wavelength into the time-evolution of the concentration of a certain component:

$$\mathbf{c}_l = \mathbf{x}_j b_{lj} \quad (3)$$

where $\mathbf{c}_l$ denotes the time-evolution of the concentration of component l, $\mathbf{x}_j$ is the jth column of the spectral matrix $\mathbf{X}$, and b_{lj} represents the calibration factor for component l at the wavelength j. Separate sets of injections are required to determine b_{lj} for each component. The CIM then employs these calibration factors to estimate $\mathbf{c}_l$ for all the components and the measured state-matrix $\mathbf{C}$ can easily be obtained by placing the column vectors $\mathbf{c}_l$ next to each other.

The next step is the availability of a model that can predict the time-evolution of the concentrations of all components, i.e. that can provide a modeled time-resolved concentration matrix $\hat{\mathbf{C}}(\mathbf{k})$, where $\mathbf{k}$ consists of p model parameters that are physicochemical or transport properties of the system, e.g. adsorption isotherm parameters or dispersion coefficients.

The classical inverse method estimates the model parameters $\mathbf{k}$ by minimizing in some sense the difference between the matrices $\hat{\mathbf{C}}(\mathbf{k})$ and $\mathbf{C}$. It is clear that this classical approach relies on a calibration procedure, which is often very time-consuming [1].

3.3. Direct inverse method

One can however also use the time-resolved UV elution spectra, i.e. the matrix $\mathbf{X}$ itself, to estimate directly the model parameters without converting explicitly the spectral matrix $\mathbf{X}$ into the measured concentrations $\mathbf{C}$. Formally, this would imply minimizing for instance the sum S_r of the squares of the elements of the residual matrix $\mathbf{R}(\mathbf{k})$ $(n \times m)$:

$$\mathbf{R}(\mathbf{k}) = \mathbf{X} - \hat{\mathbf{C}}(\mathbf{k})\mathbf{A} \quad (4)$$

where both the p elements of the vector $\mathbf{k}$ and the $d \times m$ elements of the matrix $\mathbf{A}$ are unknown and should be obtained through some optimization procedure, i.e. a rather challenging task considering that the number of elements of $\mathbf{A}$ can be large. However, using the pseudoinverse matrix of $\hat{\mathbf{C}}(\mathbf{k})$, i.e. $\hat{\mathbf{C}}^{+}(\mathbf{k}) = (\hat{\mathbf{C}}^{T}(\mathbf{k})\hat{\mathbf{C}}(\mathbf{k}))^{-1}\hat{\mathbf{C}}^{T}(\mathbf{k})$, Eq. (4) can be rewritten as:

$$\mathbf{R}(\mathbf{k}) = \mathbf{X} - \hat{\mathbf{C}}(\mathbf{k})\hat{\mathbf{C}}^{+}(\mathbf{k})\mathbf{X} = [\mathbf{I} - \hat{\mathbf{C}}(\mathbf{k})\hat{\mathbf{C}}^{+}(\mathbf{k})]\mathbf{X}. \quad (5)$$

By minimizing the sum of the squares of the elements of the residual matrix $\mathbf{R}(\mathbf{k})$ one obtains the p unknown model parameters, i.e. a much easier task than solving Eq. (4) [11,12,9,10].

This technique should not be confused with multivariate curve resolution (MCR), a technique that estimates the matrices $\mathbf{C}$ and $\mathbf{A}$ entirely through optimization without a detailed process model but using only physical constraints, e.g. concentration can not be negative and mass balances must be fulfilled [13–15].

3.4. Parameter estimation techniques

For the estimation of the parameters from the problem defined in Eq. (5), optimization algorithms such as the Newton–Gauss–Levenberg/Marquardt (NGL/M) and the simplex method approach [16] were employed using the *lsqnonlin* and *fminsearch* functions in MATLAB, respectively. The sensitivity of the obtained parameters is indicated by their confidence intervals, i.e. the smaller the confidence interval the smaller the sensitivity of the parameter [12]. Approximate confidence intervals can be calculated using the sensitivity matrix or Jacobian based on a linearized model in the vicinity of the estimated model parameters. This sensitivity matrix enables to calculate the covariance matrix of the parameter estimates. The standard error s_i of the ith parameter k_i is given by the square root of the ith diagonal element of this covariance matrix. The confidence interval of the ith parameter is given by $k_i \pm t_{\alpha,\nu} s_i$, where $t_{\alpha,\nu}$ is the value of the t-distribution for ν degrees of freedom, i.e. the number of data points minus the number of parameters, and a confidence level of α. Here $\alpha = 0.05$ was used, thus providing a 95% probability.

4. Chromatographic model

The equilibrium-dispersive model of chromatography was used to describe the evolution of the concentration of two components over time and space, hence the mass balance for component i can be written as [1,17,18]:

$$\varepsilon^* \frac{\partial c_i}{\partial t} + (1 - \varepsilon^*) \frac{\partial q_i}{\partial t} + u \frac{\partial c_i}{\partial z} = \varepsilon^* D_{ap,i} \frac{\partial^2 c_i}{\partial z^2} \quad (i = 1, 2) \quad (6)$$

The axial dispersion and mass-transfer resistance are lumped together in an apparent dispersion coefficient term, proportional to $D_{ap,i}$. In Eq. (6), c_i and q_i are the fluid phase and the equilibrium adsorbed phase concentration, respectively. The phase equilibrium between the fluid and the adsorbed phase is characterized by the adsorption isotherm $q_i = f_i(c_1, c_2)$. The overall bed void fraction and the superficial velocity of the fluid are represented by ε^* and u, respectively. The Danckwerts boundary conditions were used to complement Eq. (6).

In this work, we follow the same numerical approach based on finite differences as done earlier [17]. The second-order space

derivative is discretized using centered differences:

$$\frac{\partial^2 c_i}{\partial z^2} = \frac{c_i(z+\Delta z) - 2c_i(z) + c_i(z-\Delta z)}{(\Delta z)^2} \quad (7)$$

with $\Delta z > 0$ representing the grid size, whereas the first-order space derivative is discretized using backward differences:

$$\frac{c_i(z) - c_i(z-\Delta z)}{\Delta z} = \left.\frac{\partial c_i}{\partial z}\right|_z - \left.\frac{\partial^2 c_i}{\partial z^2}\right|_z \frac{\Delta z}{2} + O(\Delta z^2). \quad (8)$$

The numerical error introduced by neglecting the second term on the right-hand side of Eq. (8) results in a numerical dispersion corresponding to a dispersion coefficient [1,17,18]:

$$D_{num} = \frac{u\Delta z}{2\varepsilon^*}. \quad (9)$$

For this reason, in the numerical calculations the apparent dispersion coefficients were corrected using the numerical dispersion, thus yielding:

$$\bar{D}_{ap,i} = D_{ap,i} - D_{num}. \quad (10)$$

The space grid size Δz fulfills the condition $\Delta z < 2\varepsilon^* D_{ap,i}/u$, i.e. in order to have a positive value on the left-hand side of the last equation.

In this work, both components were assumed to be subject to a competitive generalized Langmuir isotherm [19]:

$$q_i = \frac{H_i c_i}{1 + K_1 c_1 + K_2 c_2}, \quad (11)$$

where K_1 and K_2 can be either positive or negative.

5. Results and discussion

In this section, the feasibility of the proposed direct inverse method will be studied thoroughly using synthetic (first part of this section) as well as experimental data (second part of this section).

5.1. Simulation results

Let us consider two components subject to a binary adsorption isotherm as given by Eq. (11), where the corresponding isotherm parameters equal $H_1 = 10$, $H_2 = 12$, $K_1 = 0.1$ and $K_2 = 0.1$. Two chromatographic separations were simulated differing in the feed concentrations, i.e. $\mathbf{c}_f$ = [8 10] g/L and $\mathbf{c}_f$ = [20 20] g/L, where the first and second element of $\mathbf{c}_f$ represents the feed concentration of component one and two, respectively. The column characteristics were assumed to be as described in Section 2. The equilibrium-dispersive model was used and the apparent axial dispersion coefficient D_{ap} was assumed to be equal to 5×10^{-6} m^2 s^{-1} for both components.

To obtain the time-resolved UV elution spectra, i.e. to obtain the spectral matrix $\mathbf{X}$, pure-component UV spectra have to be used. First, single Gaussian (peak-shaped) functions were assumed as pure-component spectra for both components. Once the concentration profiles were calculated, the spectral matrix could easily be calculated using Eq. (2) and white noise with a standard deviation of 3 mAu was added in order to generate realistic UV elution spectra.

The time-evolution of the concentrations, the pure-component spectra, the noise and the resulting simulated UV elution spectra are shown in Fig. 2.

As discussed in Section 3.4, standard optimization algorithms can be used to solve the optimization problem associated to Eq. (5), i.e. to recover the parameter values initially selected, using UV elution spectra as shown in Fig. 2(d) and the process model to calculate the concentration matrix $\hat{\mathbf{C}}(\mathbf{k})$. Both the Newton–Gauss–Levenberg/Marquardt (NGL/M) and the simplex method resulted in the correct parameters (exactly correct to two significant digits) in case of low as well as high feed concentrations. It should be emphasized that the concentration profiles shown in Fig. 2(a) are entirely overlapping and that either a fraction analysis or a calibration at one or multiple wavelengths would have been required in order to apply the classical inverse method in this case.

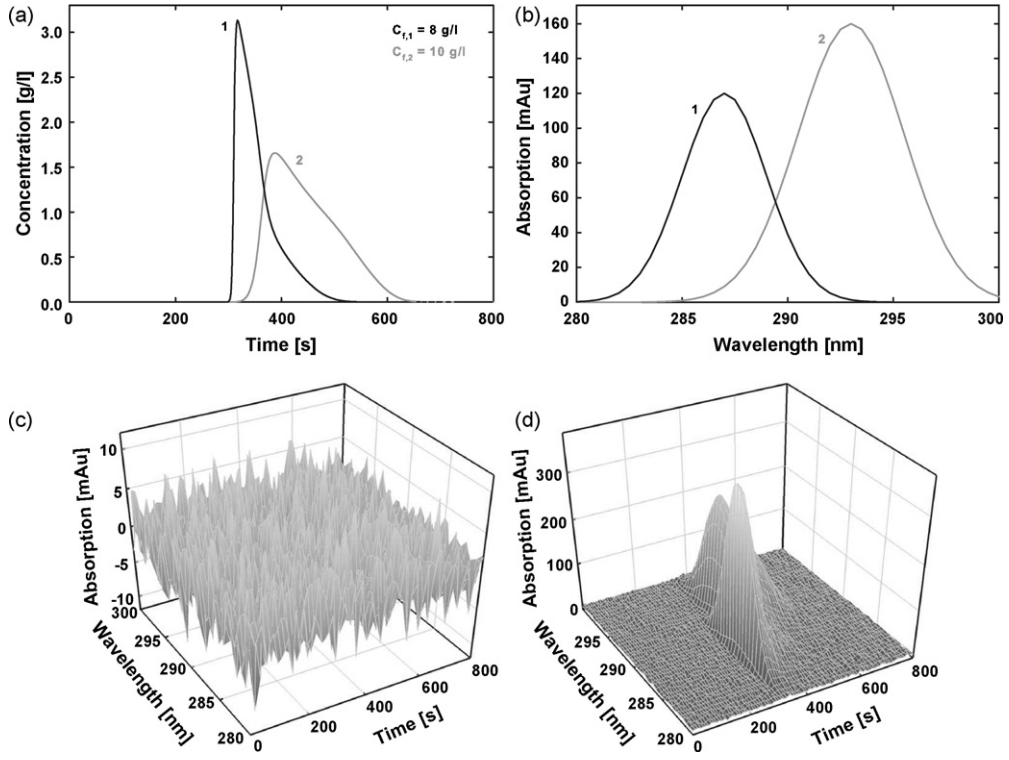

Fig. 2. The time-evolution of the concentrations (a), the pure-component spectra (b), the noise (c) and the resulting simulated UV elution spectra (d) used in the simulation studies in the case of Gaussian pure-component spectra.

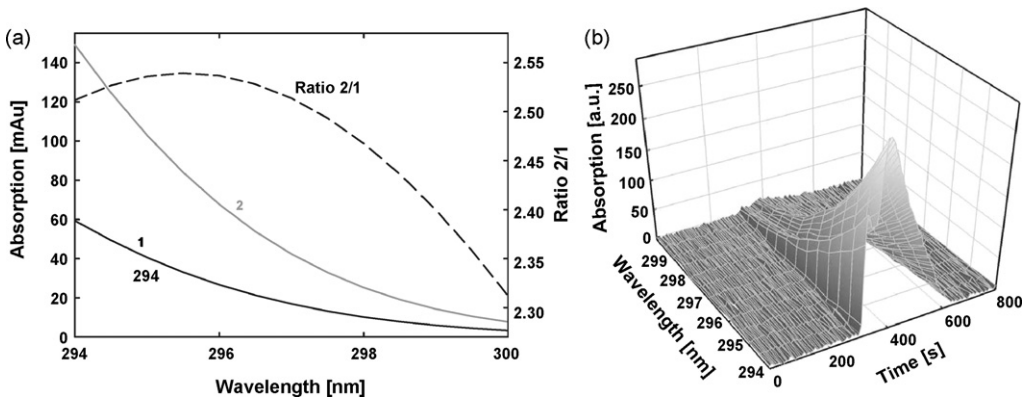

Fig. 3. The pure-component spectra (a) and the resulting simulated UV elution spectra (b) used in the simulation studies in the case of more realistic pure-component spectra. To show that the pure-component spectra are indeed different, the ratio of both has also been plotted (dashed line).

Table 1
Experimental conditions of the different runs. All experiments were performed at 22 °C. The first element of the feed concentration $\mathbf{c}_f$ represents the feed concentration of phenetole (component 1).

Run	Feed concentration [g/L]	Injection volume [μL]
1	[10 15]	5
2	[10 15]	20
3	[10 15]	35
4	[6 9]	15
5	[6 9]	50
6	[6 9]	60

It is well-known however, that pure-component UV spectra do not resemble Gaussian (peak-shaped) functions and the range of wavelengths where the intensity scales linearly with the concentration is usually found in the tails of the UV signals. Hence the same procedure was carried out using the pure-component spectra shown in Fig. 3(a). To demonstrate that the two pure-component spectra are indeed different, the ratio of both has also been plotted. The resulting simulated UV elution spectra in the case of the low feed concentrations are shown in Fig. 3(b). It is worth noting that the time-evolution of the concentrations and the noise were the same as in the case of Gaussian (peak-shaped) functions. Also in this case, the Newton–Gauss–Levenberg/Marquardt (NGL/M) and the simplex method resulted in the correct parameters (exactly correct to two significant digits) for both low and high feed concentrations.

5.2. Experimental results

Six different experiments were performed using different feed concentrations and injection volumes; the corresponding experimental conditions are reported in Table 1. The elution profiles of runs 1–3 and of runs 4 to 6 are shown in Fig. 4(a) and (b), respectively. As it can readily be seen, runs 1 and 4 exhibit baseline separation, whereas runs 2 and 5 exhibit moderate overlapping and runs 3 and 6 complete overlapping of the two components.

In this section, all runs are analyzed both through the classical inverse method using the concentration profiles, i.e. obtained either from the elution profiles through a calibration or from the outcome of a fraction analysis, and through the direct inverse method using the absorption profiles only. In the first part, three different sets of runs are considered independently, i.e. runs 1 and 4, runs 2 and 5 and runs 3 and 6. In the second part, all runs will be used together to estimate the adsorption isotherm parameters and the axial dispersion coefficients using the classical and the direct inverse method.

It is worth noting that while on the one hand K_2 is positive, indicating that 4-*tert*-butylphenol (component 2) follows a Langmuir isotherm, on the other hand K_1 was found to be negative, meaning that phenetole (component 1) is subject to an anti-Langmuir isotherm. As a consequence, this specific binary system is subject to the mixed generalized Langmuir isotherm M_2 as introduced earlier [19].

Fig. 5(a) and (c) show the experimental (symbols) and simulated (lines) concentration profiles in the case of runs 1 and 4, respectively. The estimated adsorption isotherm parameters and dispersion coefficients, i.e. the results of the classical inverse method, are given in the left column of the first part of Table 2. Fig. 5(b) and (d) display the experimental (symbols) and simulated (lines) absorption profiles for three different wavelengths in the case of runs 1 and 4, respectively. The estimated adsorption isotherm parameters and dispersion coefficients, i.e. the results of the direct inverse method, are given in the right column of the

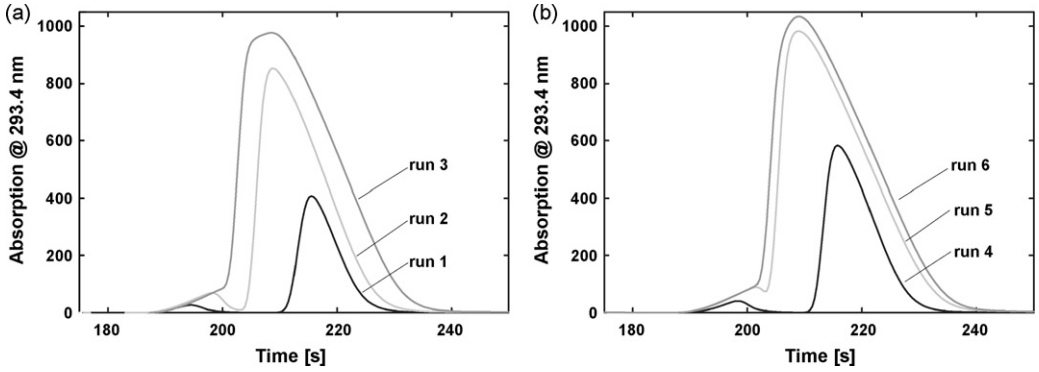

Fig. 4. The absorption profiles for runs 1–3 (a) and for runs 4–6 (b). All experiments were performed at 22 °C.

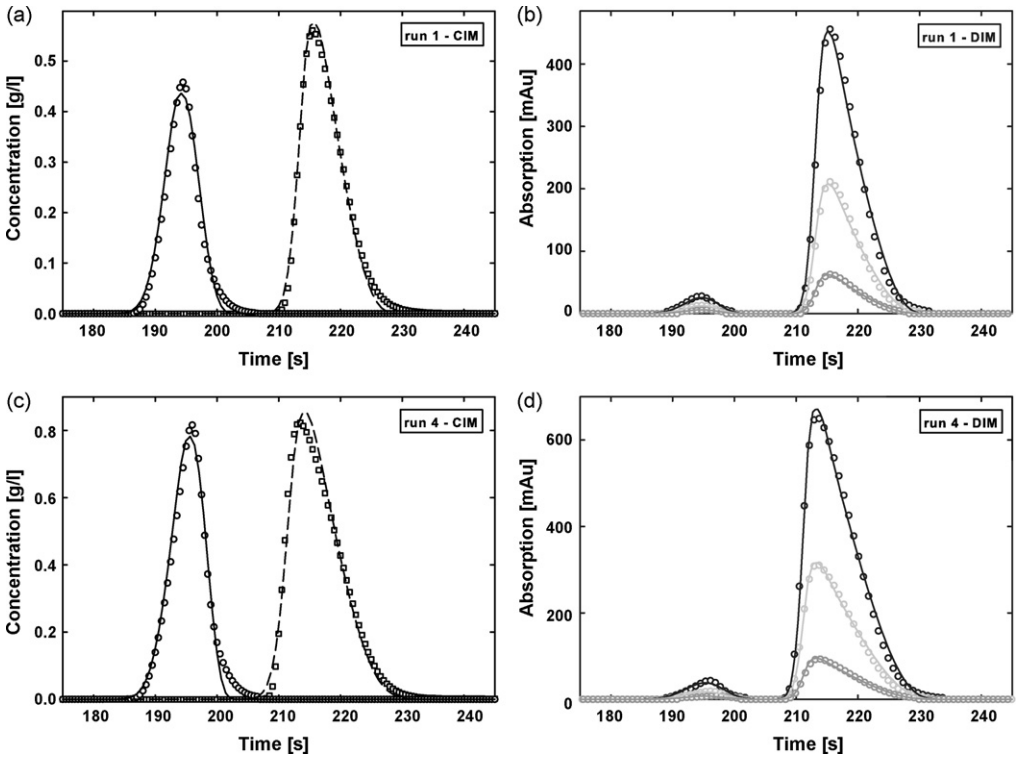

Fig. 5. The results of the classical and the direct inverse method in the case of run 1 (a and c) and run 4 (c and d). The intensities at wavenumbers 292 (highest intensity), 295 and 297 (lowest intensity) nm are plotted.

first part of Table 2. As it can be seen, the differences between the parameters estimated through the classical and the direct inverse method are small, which demonstrates the potential of the new calibration-free method. Note also that $D_{ap,1} \neq D_{ap,2}$.

The same sequence of figures is shown in Figs. 6 and 7 in the case of runs 2 and 5 and in the case of runs 3 and 6, respectively. An important difference with respect to runs 1 and 4 is that the concentration profiles, required to apply the classical inverse method, can not be obtained from the absorption profiles and the calibration because the peaks are overlapping, hence the concentration profiles were obtained using fraction analysis, i.e. a tedious and time-consuming experimental procedure. The estimated adsorption isotherm parameters and dispersion coefficients are reported in the second and third part of Table 2. As it can be seen, even when the compounds are entirely overlapping, very similar parameter values can be obtained using the direct inverse method, i.e. with neither calibration nor fraction analysis.

Of course all runs can be used together to provide a final estimate for the adsorption isotherm parameters using the classical and direct inverse method. The parameter values of this analysis are reported in Table 3. For reasons of clarity, the estimates for the dispersion coefficients are not given as they were very similar to those given in Table 2. As it can be seen, both sets of parameters are very similar and will result in very similar adsorption isotherms.

It is worth noting, that there is always a small discrepancy between the estimated parameter values using the classical and the direct inverse method. However, in the case of the dispersion coefficients, the discrepancy between the two approaches is relatively large, especially in the cases where fraction analysis was required to determine the concentration profiles. In the latter case additional tubing was required which introduced additional dispersion in the system that is not present in the adsorption profiles measured by the UV detector. This additional dispersion is inevitable and results in slightly longer tails in the chromatograms and hence in larger values of the dispersion coefficients.

Table 2
Results of the classical and the direct inverse method using three different sets of experimental data. All optimizations were performed using the simplex algorithm. The values for the dispersion coefficients are given in 10^{-5} m^2 s^{-1} For reasons of clarity, the subscript *ap* has been omitted for the dispersion coefficients.

		Classical inverse method	Direct inverse method
Runs 1 and 4	H_1	1.79 ± 0.01	1.80 ± 0.01
	H_2	2.25 ± 0.01	2.27 ± 0.01
	K_1	−0.011 ± 0.001	−0.012 ± 0.001
	K_2	0.035 ± 0.003	0.045 ± 0.004
	D_1	2.74 ± 0.02	2.20 ± 0.02
	D_2	2.19 ± 0.05	2.46 ± 0.03
Runs 2 and 5	H_1	1.85 ± 0.03	1.83 ± 0.01
	H_2	2.31 ± 0.03	2.29 ± 0.02
	K_1	−0.019 ± 0.007	−0.016 ± 0.004
	K_2	0.042 ± 0.009	0.042 ± 0.008
	D_1	6.95 ± 0.08	2.98 ± 0.06
	D_2	9.90 ± 0.06	6.60 ± 0.05
Runs 3 and 6	H_1	1.89 ± 0.01	1.88 ± 0.01
	H_2	2.27 ± 0.04	2.30 ± 0.02
	K_1	−0.019 ± 0.009	−0.019 ± 0.005
	K_2	0.041 ± 0.009	0.044 ± 0.006
	D_1	9.95 ± 0.07	9.56 ± 0.05
	D_2	15.88 ± 0.09	10.55 ± 0.07

Table 3
Results of the classical and the direct inverse method using all runs at the same time. All optimizations were performed using the simplex algorithm.

		Classical inverse method	Direct inverse method
Runs 1–6	H_1	1.84 ± 0.01	1.83 ± 0.01
	H_2	2.27 ± 0.02	2.28 ± 0.01
	K_1	−0.018 ± 0.009	−0.017 ± 0.007
	K_2	0.041 ± 0.008	0.043 ± 0.006

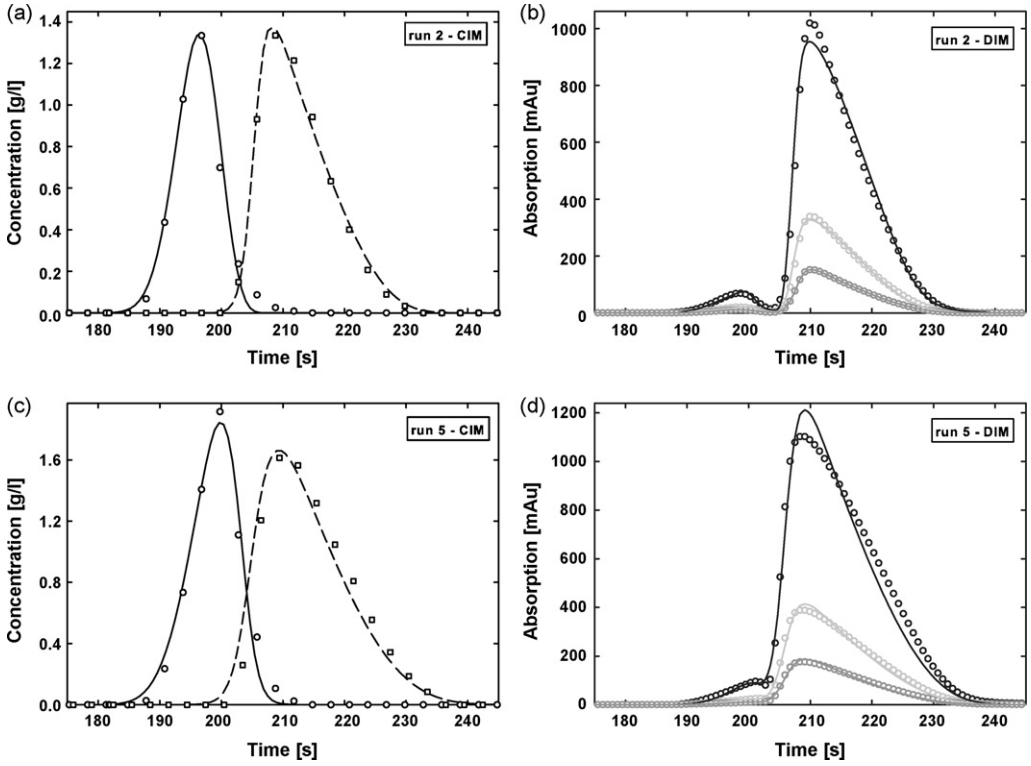

Fig. 6. The results of the classical and the direct inverse method in the case of run 2 (a and c) and run 5 (c and d). The concentration values in the parts a and c were obtained using a fraction analysis. The intensities at wavenumbers 292 (highest intensity), 295 and 297 (lowest intensity) nm are plotted.

5.3. Discussion

The novel direct inverse method has proven to be capable of estimating the adsorption isotherm parameters with the same accuracy as the classical inverse method. This result has two important implications: the first is the elimination of the conversion of a measured absorption value into a concentration value, i.e. the elimination of the calibration and of the need for pure species. The

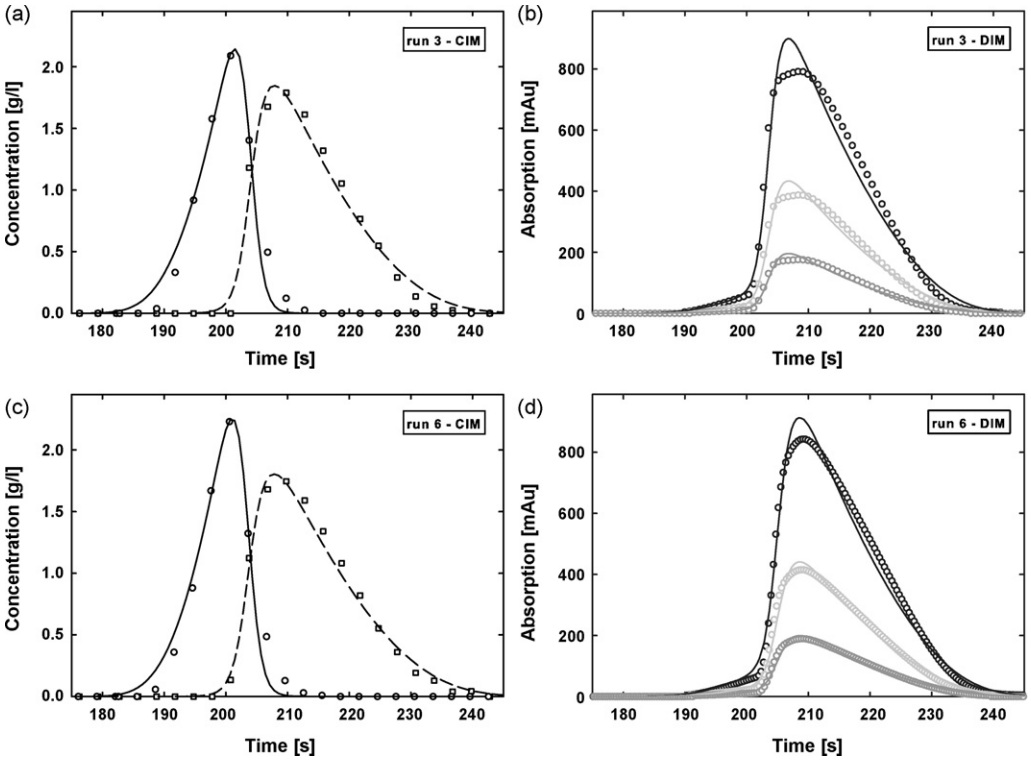

Fig. 7. The results of the classical and the direct inverse method in the case of run 3 (a and c) and run 6 (c and d). The concentration values in the parts a and c were obtained using a fraction analysis. The intensities at wavenumbers 293 (highest intensity), 296 and 298 (lowest intensity) nm are plotted.

second is the elimination of fraction analysis in the case of overlapping signals, which will save a significant amount of experimental work and resources.

A couple of remarks are worth making. First, the estimated parameter values do not depend on their initial guesses, whose choice influences at most the duration of the calculation. It is worth noting that the best estimate for K_1 turned out always to be negative, whatever the sign of its initial guess. Second, the parameters were in our calculations unconstrained, i.e. there were no boundaries on the unknown parameters. However, it is possible to constrain the search in order to fulfill specific physical requirements. Third, the Henry constants are also estimated in this work through both the direct and classical inverse method. It is well-known however, that their values can be measured also through analytical pulse injections. The values for the Henry constants could then be fixed in the optimization problem, thus leaving the equilibrium constants and the dispersion coefficients only to be estimated and shortening the computation time.

The applicability of the newly proposed method hinges on the linearity of the detector's response. This is not the major limitation that it might look like for at least two reasons. First, in the case of UV absorbance, which is of course the most important case, there is a range of wavelengths that scale linearly with concentration for many chemical species. This is normally enough for an effective application of the method. Secondly, a few measurements with the mixture available at different overall concentrations, e.g. different dilutions, would suffice to better identify and thoroughly verify the existence and location of this linear region.

Therefore, we believe that the newly proposed method is a valuable addition to the portfolio of available techniques to estimate the adsorption isotherms of a multi-component mixture, particularly when the availability of the pure substances is limited. This is a challenging task for chromatographers, and the availability of alternative strategies to accomplish it can only be advantageous for chromatography practitioners.

Nomenclature

b	calibration factor [$g\,L^{-1}\,mAu^{-1}$]
c	concentration [$g\,L^{-1}$]
D	dispersion coefficient [$m^2\,s^{-1}$]
H	Henry coefficient
$\mathbf{k}$	vector of model parameters
K	equilibrium constant [$L\,g^{-1}$]
L	length of the column [m]
p	number of unknown parameters
q	equilibrium adsorbed phase concentration [$g\,L^{-1}$]
s	standard error
t	time [s]
u	superficial velocity [$m\,s^{-1}$]
z	space coordinate [m]
$\mathbf{A}$	pure-analyte spectra matrix
$\mathbf{C}$	concentration matrix
$\mathbf{E}$	matrix of measurement errors
$\mathbf{R}$	residual matrix
$\mathbf{X}$	spectral matrix

Greek letter

ε^*	overall bed void fraction

References

[1] G. Guiochon, A. Felinger, D.G. Shirazi, A.M. Katti, Fundamentals of Preparative and Nonlinear Chromatography, 2nd ed., Academic Press, New York, 2006.
[2] I. Quinones, J.A. Ford, G. Guiochon, Anal. Chem. 72 (7) (2000) 1495.
[3] A. Felinger, A. Cavazzini, G. Guiochon, J. Chromatogr. A 986 (2) (2003) 207.
[4] W. Piatkowski, D. Antos, F. Gritti, G. Guiochon, J. Chromatogr. A 1003 (1–2) (2003) 73.
[5] S. Abel, G. Erdem, M. Amanullah, M. Morari, M. Mazzotti, M. Morbidelli, J. Chromatogr. A 1092 (2005) 2.
[6] P. Forssen, R. Arnell, T. Fornstedt, Comput. Chem. Eng. 30 (9) (2006) 1381.
[7] N. Marchetti, A. Cavazzini, L. Pasti, F. Dondi, J. Sep. Sci. 32 (5–6) (2009) 727.
[8] R. Arnell, P. Forssen, T. Fornstedt, J. Chromatogr. A 1099 (1–2) (2005) 167.
[9] J. Cornel, M. Mazzotti, Anal. Chem. 80 (23) (2008) 9240.
[10] J. Cornel, M. Mazzotti, Ind. Eng. Chem. Res. 48 (23) (2009) 10740.
[11] M. Maeder, A.D. Zuberbuhler, Anal. Chem. 62 (20) (1990) 2220.
[12] G. Puxty, M. Maeder, K. Hungerbuhler, Chemometrics Intell. Lab. Syst. 81 (2) (2006) 149.
[13] J. Diewok, A. de Juan, M. Maeder, R. Tauler, B. Lendl, Anal. Chem. 75 (3) (2003) 641.
[14] R. Tauler, B. Kowalski, S. Fleming, Anal. Chem. 65 (15) (1993) 2040.
[15] R. Tauler, Chemometrics Intell. Lab. Syst. 30 (1) (1995) 133.
[16] W. Press, S.A. Teukolsky, W. Vetterling, Numerical Recipes in Fortran, Cambridge University Press, Cambridge, 1992.
[17] S. Katsuo, C. Langel, P. Schanen, M. Mazzotti, J. Chromatogr. A 1216 (7) (2009) 1084.
[18] C. Migliorini, A. Gentilini, M. Mazzotti, M. Morbidelli, Ind. Eng. Chem. Res. 38 (6) (1999) 2400.
[19] M. Mazzotti, Ind. Eng. Chem. Res. 45 (15) (2006) 5332.